VOLTAGE CLAMP OF CARDIAC MUSCLE

A THEORETICAL ANALYSIS OF EARLY CURRENTS IN THE SINGLE SUCROSE GAP

J. MAILEN KOOTSEY *and* EDWARD A. JOHNSON

From the Department of Physiology and Pharmacology, Duke University Medical Center, Durham, North Carolina 27710

ABSTRACT A theoretical model is presented for the early currents in the voltage clamp of cardiac muscle using the single sucrose gap technique. The preparation is represented by a single one-dimensional active cable with modified Hodgkin-Huxley membrane and the interent imperfections in the technique are also included, e.g., leakage through the sucrose gap and resistance in series with the membrane in the test compartment. The stability of the control system was found to depend on the position of the control point with respect to the sucrose gap border. Computed currents for a stable system closely resembled those in the literature and those from a near-ideal system (e.g., squid axon.) The potential immediately across the membrane, however (not including potential drops across the series resistance external to the membrane), was found to be essentially uncontrolled and the "current-voltage" relationship was shown to be almost independent of membrane properties.

INTRODUCTION

Many of the recent attempts to voltage clamp cardiac muscle have used either the single or double sucrose gap methods. Because of the size and complexity of the preparation used, there are good intuitive reasons to question the interpretations put on these data (Johnson and Lieberman, 1971). Instead of a single short cylinder of membrane, we are attempting to control the potential in, at best, a segment containing 1 or more thousand parallel-aligned, interconnected fibers of some 10 or more cell diameters in length. Two consequences of this make the application of the single and double sucrose gap particularly difficult. First, an adequate sucrose gap has to be established about all the fibers in the preparation, regardless of their position in the bundle. Secondly, the electrical length of the segment is a severe handicap in assuring adequate uniformity of membrane potential at all times of interest.

In order to explore more rigorously the nature and severity of the limitations imposted by these difficulties, we have begun a detailed theoretical analysis of these

two methods of voltage clamp. Our aim has been to develop a model incorporating what is known about the preparation and method, but with the minimum degree of complexity necessary to fit the published experimental results. Previous analyses of the difficulties encountered in the voltage clamp method have centered around a single patch of membrane or a two-patch membrane, one patch with and one without a resistance in series with the membrane (Taylor et al., 1960; Chandler et al. 1962; and McAllister, 1968). The present paper describes the results from a model applied to early currents observed with a single sucrose gap clamp in which the active, membrane is distributed in the form of a cylinder.

THE THEORETICAL MODEL

The preparation that has been used for the sucrose gap clamp has been a trabecula of mammalian ventricular muscle. Typical relevant dimensions are an over-all diameter of less than 0.7 mm, and a length of 1 mm in the test chamber (Beeler and Reuter, 1970; Mascher and Peper, 1969; Ochi, 1970). Preparations from the sheep and dog have a similar structure. The fibers are 10–15 μ in diameter and except where the fibers form junctional complexes, the cells are relatively wide apart so that little if any membrane should be in series with an external resistance. Although these fibers, like skeletal muscle, have a transverse tubular system, the tubules are much shorter ($\sim$5 μ) and of larger diameter ($\sim$2000 A) so that they are short in comparison with their length constant (length constant λ = 100 μ, assuming a specific membrane resistance of 1000 ohm-cm^2 and core resistivity of 50 ohm-cm) and can be neglected to a good approximation.

Fig. 1 A illustrates what is probably the simplest model that might be thought to represent the preparation and method of clamp. The ventricular trabecula is represented by a cylindrical cable with complex membrane properties. Controlling current is injected at one end of the cable and the membrane potential is measured

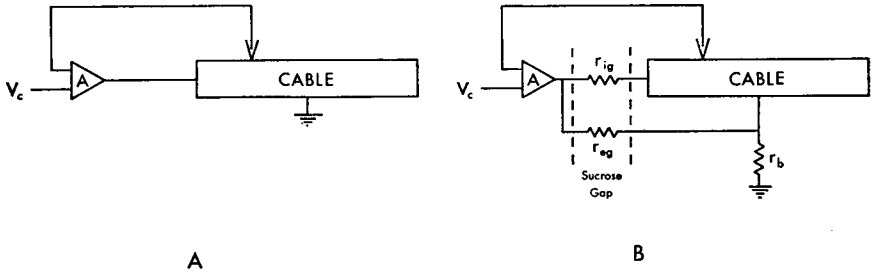

FIGURE 1 (A) Basic model of the single sucrose gap voltage clamp system. Amplifier A supplies control current to the end of the cable, the magnitude of the current depending on the difference between the command voltage V_c and the voltage measured by the intracellular microelectrode. (B) Voltage clamp model of the single sucrose gap modified to incorporate the intracellular axial resistance r_{ig}, the sucrose leakage resistance r_{eg}, and the membrane series resistance r_b.

somewhere along the cable in the test compartment, where it is assumed that there is zero resistance in extracellular space. The electronics consists of an error amplifier with finite gain and bandwidth.

This simplified model represents a negative feedback control circuit, where the membrane voltage of the cable is the parameter being controlled. When such a model was perturbed from resting potential, it was found to oscillate. This is to be expected since propagation time along the cable between the point of injection of current and the point at which the voltage is measured appears in the feedback loop as a fixed delay time. In order for such a feedback circuit to be stable when the loop is closed, the response time of the control amplifier (and also of the closed-loop system) must be long in comparison with the delay time in the cable (see Appendix). If this is not the case, the system goes into oscillation with a period roughly equal to the cable delay. A passive RC cable exhibits a propagation velocity of the half-amplitude point of $2\lambda/\tau$ (Hodgkin and Rushton, 1946) where τ is the membrane time constant. Taking a length of 1 mm as typical of the preparation used in the single sucrose gap method and a propagation velocity of 0.5 m/sec as typical of mammalian ventricular muscle, the delay time between the ends of the preparation is 2 msec. Thus, if the membrane potential were measured at the far end of the cable, the closed-loop response time would have to be around 10 msec for stability. In order to achieve an apparent rise time of 50 μsec, the voltage-measuring point would have to be approximately 10 μ from the sucrose gap border; however, published reports have indicated stability with a speed of response in the submillisecond range without the need for positioning of the voltage electrode very close to the sucrose gap. Thus it is reasonable to conclude that the model in Fig. 1 A is an oversimplification.

Modifications to the model need not be arbitrary, for the nature of the method and published reports suggest two additional complications. It is well known that the sucrose gap is an imperfect insulator and that a significant fraction of the recorded current flows through the sucrose in extracellular space (New, 1971). Secondly, Beeler and Reuter (1970) found that there was a resistance of about 500 ohms in series with the membrane in their preparation. Although both the membrane series resistance and sucrose gap leakage are distributed resistances, we have represented them as lumped resistances as a first approximation. For the sake of simplicity in the model, the likely stray capacitances have been omitted; however, their effects, which can be surmised from the results, will be discussed later. Fig. 1 B shows the expanded model from which the following results were obtained.

If the preparation consisted of a bundle of fibers of identical diameter and membrane properties and if current were injected uniformly into all fibers at one end, then the electrical behavior of all the fibers would be identical. The presence or absence of low resistance interconnections between fibers would be of no consequence provided that the area of membrane involved in such junctions did not significantly reduce the active membrane area. If there were differences between the fibers, then the interconnections would tend to average the effects over the whole population of

fibers, but a fiber in the bundle could still be represented as a single cylindrical cable. The frequency and distribution of probable resistive connections between the fibers in such a trabecula have not been investigated. Alhough the interconnections are probably similar to those found in a tiny trabecula in the rabbit heart (Johnson and Sommer, 1967), we nevertheless represented the preparation as a single one-dimensional cable, the electrical behavior of which is described by the following partial differential equation:

$$\frac{1}{r_i}\frac{\partial^2 V_m}{\partial x^2} = i_m = C_m\frac{\partial V_m}{\partial t} + i_i, \qquad (1)$$

where V_m is the transmembrane potential and varies with time t and distance x along the cable axis. i_m is the membrane current per unit length made up of the ionic current i_i per unit length and the current through a capacitance c_m per unit length. r_i is the resistance of the cytoplasm per unit length and is assumed to be constant.

We have made use of the Hodgkin-Huxley formulation (Hodgkin and Huxley, 1952) to describe the ionic currents during the depolarization phase of the cardiac action potential. All available evidence to date suggests that the depolarization phase of the cardiac action potential results from a sodium-carrying mechanism similar to that in the squid axon (Weidmann, 1955). Immediate repolarization was prevented by eliminating the delayed rise in potassium conductance. The resultant wave form of the propagated action potential is shown in Fig. 2. Although this is a crude approximation to a cardiac action potential, it served our purpose and made it unnecessary

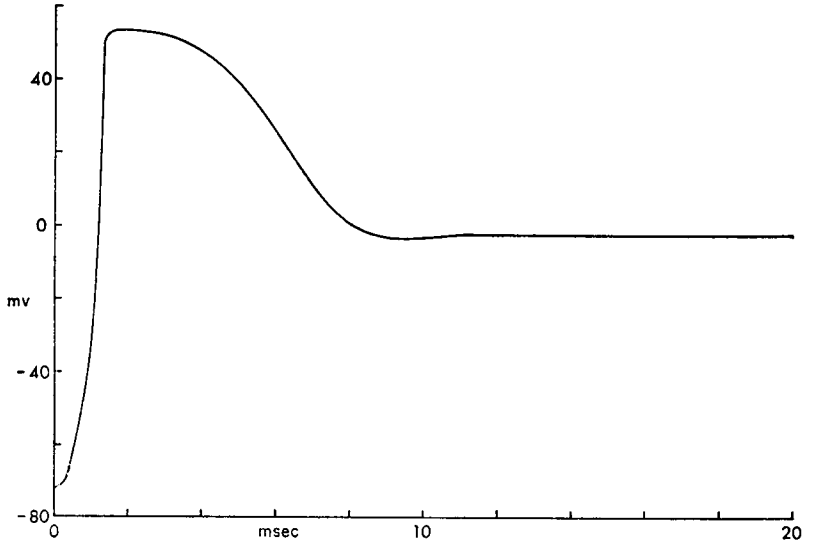

FIGURE 2 Computed wave form of the propagated action potential initiated from the sucrose gap border and recorded from segment 4 of the unclamped cable.

to make further assumptions which would complicate the interpretation of our results.

The voltage control system was represented as a differential amplifier with a constant gain G up to a frequency of $0.35/\tau$ and a roll-off of 6 db/octave above that frequency. Such an amplifier has a voltage output V_A governed by the differential equation

$$\frac{dV_A}{dt} = \frac{G}{\tau} V_{in} - \frac{1}{\tau} V_A , \tag{2}$$

where V_{in} is the net input voltage. If V_p is the transmembrane potential at the point being controlled, V_1 is the transmembrane potential at the sucrose gap border, and V_C is the command potential, the differential equation governing V_A in the closed-loop configuration is

$$\frac{dV_A}{dt} = -\frac{1}{\tau}\left[1 + \frac{Gr_b}{r_b + \dfrac{r_{eg}r_{ig}}{r_{eg} + r_{ig}}}\right] V_A + \frac{G}{\tau}(V_C - V_p) + \frac{G}{\tau} \frac{\dfrac{r_{eg}r_b}{r_{eg} + r_b}}{r_{ig} + \dfrac{r_{eg}r_b}{r_{eg} + r_b}} V_1 . \tag{3}$$

The entire system, including the trabecula and the control electronics, is thus described by equations 1 and 3 together with the Hodgkin-Huxley equations for the ionic current, modified as above. Solutions for this system of nonlinear equations were obtained by digital computer methods. The length of the cable was divided into 21 equal segments and the difference equation equivalent to equation 1 was written and solved, together with the Hodgkin-Huxley equations for i_i, for each of the interior points by implicit matrix methods (Mitchell, 1969; Gerald, 1970). Separate equations were written for the two end segments and, together with equation 3, were integrated by the Adams-Moulton method (Gerald, 1970) to provide boundary conditions for the matrix solution. Running time on an XDS Sigma 5 (Xerox Data Systems, El Segundo, Calif.) was approximately 1 min/msec of problem time.

RESULTS

Using the model described above for the preparation and voltage clamp system, solutions were obtained for a variety of depolarizing and hyperpolarizing steps in command potential and the following values for the other parameters:

Fiber diameter = d = 10 μ.

Cytoplasmic resistivity = R_i = 150 ohm-cm.

Sucrose gap leakage resistance = r_{eg} = 7.6×10^7 ohms.

Intracellular axial resistance in sucrose gap = $r_{ig} = 3.8 \times 10^7$ ohms.
Resistance in series with membrane in test compartment = $r_b = 1.65 \times 10^6$ ohms.
Membrane specific capacitance = $C_m = 2\ \mu F/cm^2$.
Sodium equilibrium potential = $V_{NA} = +55$ mv.
Potassium equilibrium potential = $V_K = -72$ mv.
Maximum sodium conductance = $g_{NA} = 120$ mmho/cm^2.
Potassium conductance = $g_K = 0.36$ mmho/cm^2.
Spatial increment = $\Delta x = 0.005$ cm.
Time increment = $\Delta t = 0.0025$ msec.
Amplifier gain = $G = 1000$.
Amplifier time constant = $\tau = 1$ msec.
Amplifier maximum output voltage = 10 v.

The value for the fiber diameter is typical for mammalian ventricular fibers and R_i was taken from Weidmann (1952). r_{ig} was calculated from R_i by calculating the total axial resistance of a 200 μ length of a cylindrical cell 10 μ in diameter. r_{eg} was set equal to 2 r_{ig}, a typical ratio for the sucrose gap technique (New, 1971). r_b was scaled to represent 500 ohms or 2 mmho of conductance in series with every square centimeter of membrane in the test compartment (Beeler and Reuter, 1970).[1] The value for C_m was chosen to be close to the value of 2.24 $\pm$0.14 μF/cm^2 calculated for the surface sarcolemma of skeletal muscle where few assumptions are made about the membrane geometry (Gage and Eisenberg, 1969). The Hodgkin-Huxley model was the source of values for the conductances and equilibrium potentials; the resting potential was arbitrarily selected and the constant potassium conductance was set as low as possible consistent with a stable resting potential. The amplifier gain and time constant were chosen to produce an error and rate of rise in the measured potential at the point being controlled comparable to that in the literature (Beeler and Reuter, 1970). While G and τ were chosen to fit the experimental results, the values arrived at describe a realistic operational amplifier with a gain-bandwidth product of 0.3 MHz.[2] These two parameters were, in fact, the only parameters that could be considered adjustable in this model.

The stability problem associated with the propagation delay still remained, although it was not as serious as that associated with the simple model of Fig. 1 A. It was found by trial and error that stability and sufficient speed were achieved by

[1] Assuming that 25% of the total volume of Beeler and Reuter's (1970) preparation was occupied by extracellular space and taking values of 1 mm for the length of the preparation and 0.65 mm for its over-all diameter, their preparation would represent 1 cm^2 of membrane if filled with cylindrical fibers 10 μ in diameter. This value is in agreement with the area calculated from the measured value of the total membrane capacitance in the preparation and the author's estimate of specific membrane capacitance.

[2] A higher gain-bandwidth product could have been chosen, but the only benefit would have been an increase in the *apparent* (see later this section) speed of response to a clamp step at the expense of increased computer time. In practice, achieving a higher gain-bandwidth product requires special precautions with respect to stray capacitances (see end of this section).

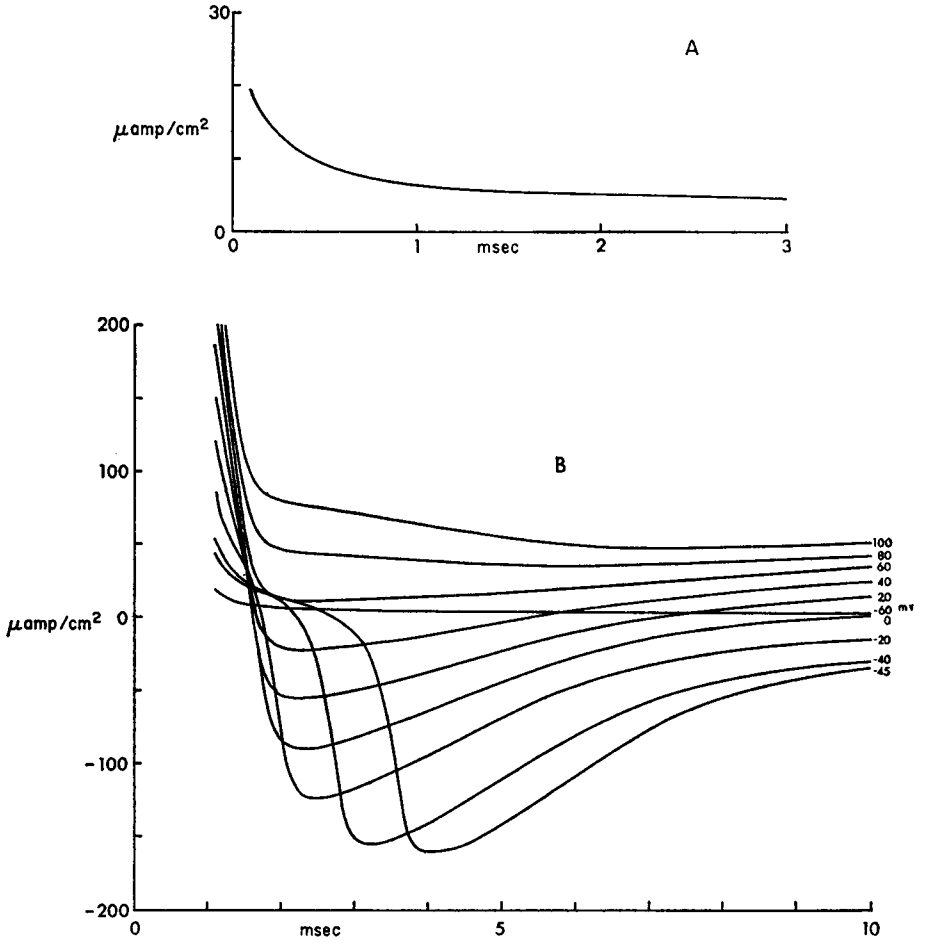

FIGURE 3 (A) Control current for a small (12 mv) depolarizing step in V_c. (B) Control currents for a series of increasing depolarizing steps in V_c.

moving the voltage sensing point about five-sixths of the way toward the sucrose gap border from the end of the 1 mm preparation.

Fig. 3 A shows the current associated with a small subthreshold depolarizing step in command potential, a response very similar to that reported by Beeler and Reuter (1970). The time constant of delay is slightly shorter, but the agreement in peak magnitude and form is excellent.

Fig. 3 B is a family of current traces associated with larger depolarizing steps in command potential. Although the sizes of the steps are not the same, the shapes and magnitudes of the curves are in excellent agreement with the experimental results of Beeler and Reuter (1970).

A plot of the peak early current (referred to zero current) as a function of the

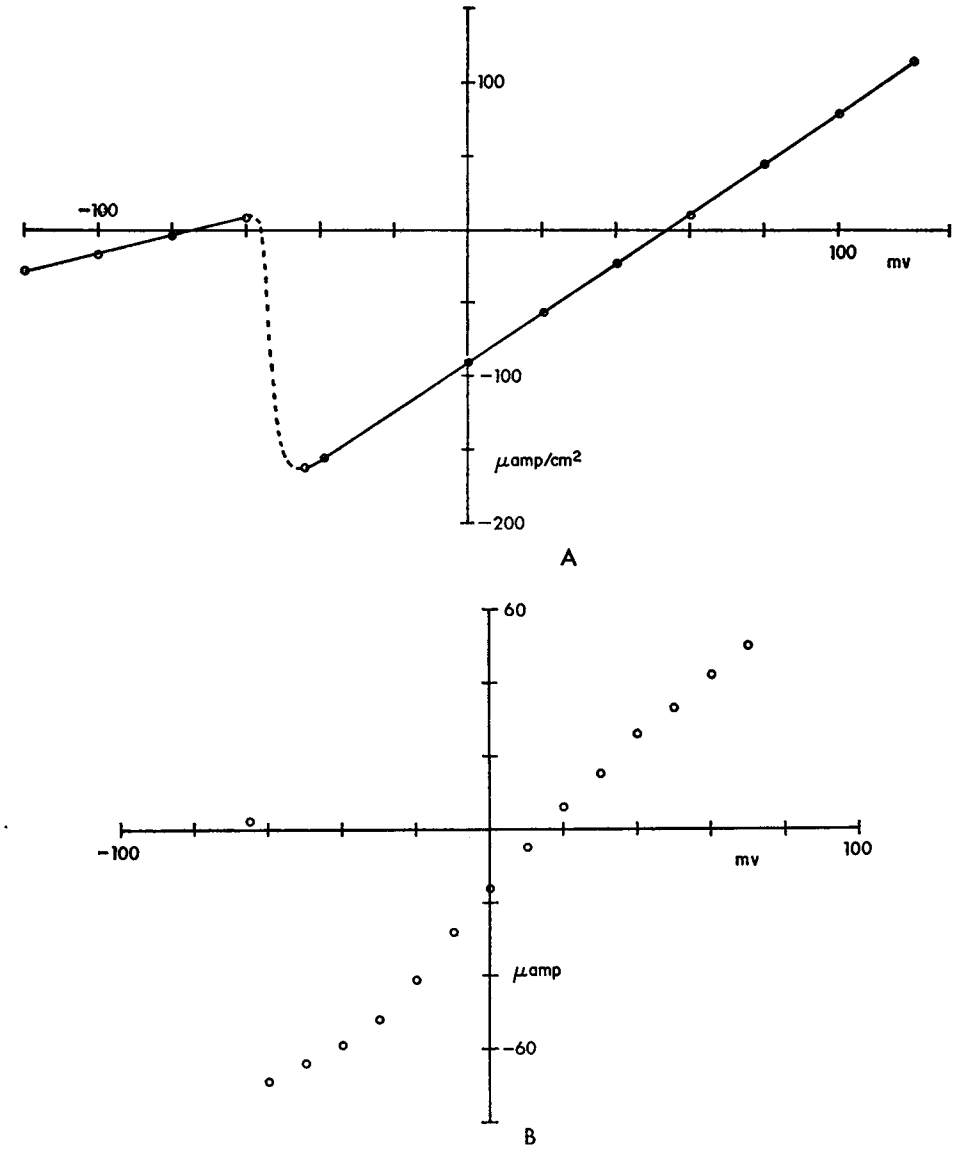

FIGURE 4 (A) Peak current-voltage plot for the records in Fig. 3 B. (B) Current-voltage plot from the results of Beeler and Reuter (1970) replotted as described in the text.

command potential is shown in Fig. 4 A. The main difference between this plot and the result of Beeler and Reuter is the curvature at large depolarizations. This curvature is almost certainly attributable to a difference in the steady-state current-voltage relationship because, in their plot, the currents are not referred to zero current, but rather to the corresponding steady-state current. By use of their steady-state current-

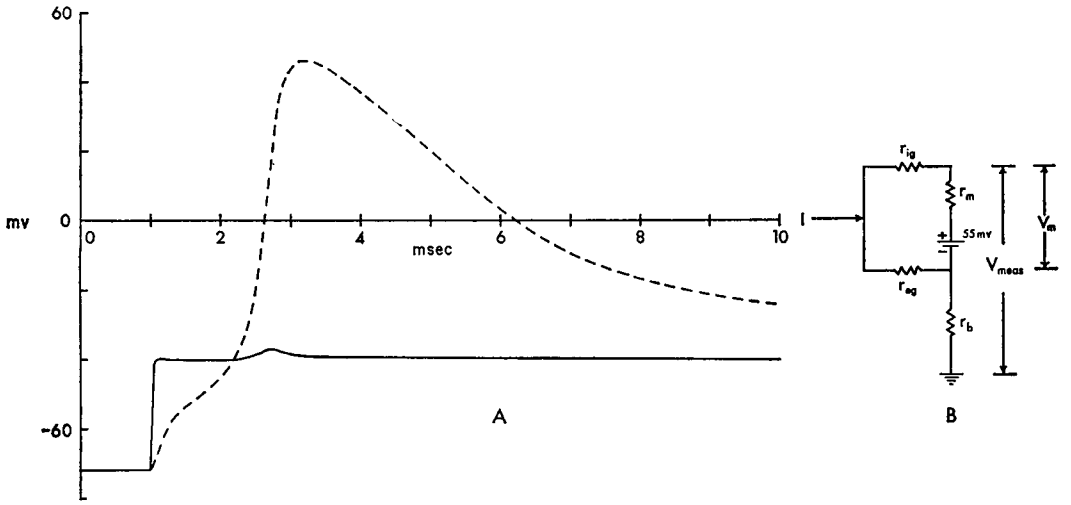

FIGURE 5 (A) Measured (V_{meas}) and true (V_m) transmembrane potentials in response to a 30 mv step in V_c. Solid line: V_{meas}, the potential between segment 3 and ground (including the potential drop across r_b). Dotted line: V_m, the potential immediately across the membrane of segment 3. (B) Lumped equivalent circuit of the preparation at peak current. The membrane at this time is represented by the 55 mv sodium battery and membrane resistance r_m. The current I is adjusted by the control amplifier to make the voltage V_{meas} follow the control voltage. Resistances r_{eg}, r_{ig}, r_b are defined in the caption to Fig. 2.

voltage relationship, we have converted their values to absolute currents (referred to zero current) and replotted them in Fig. 4 B. Their peak current-voltage relationship, plotted in this fashion, is essentially a straight line.

At this point we can exploit the advantage of the theoretical model to answer the question, What is the true transmembrane potential, i.e. the potential immediately across the membrane, not including the potential drops within the resistor r_b, and how does it compare with the measured "membrane potential"? Furthermore, we can answer questions concerning the uniformity of membrane potential control throughout the preparation since the true transmembrane potential is known for the entire length of the cable.

Fig. 5 A shows the response of the controlled internal potential to be a step in command potential. The controlled potential deviates from the command potential only during peak current and then by only about 2 mv. The remaining theoretical curve is the *true* transmembrane potential which, as can be seen, is essentially an uncontrolled action potential. The command step initiated an action potential at the sucrose gap border which propagated out of control past the recording point to the end of the preparation (see Figs. 6 A and 7 A).

The question then arises, What is the significance of the peak current-voltage plot under these circumstances? The peak current is recorded when the action potential propagates past the recording site. The situation at peak current is described by the

equivalent circuit shown in Fig. 5 B. The membrane at the peak of the action potential is represented by a battery and resistor, the battery voltage being the amplitude of the spike and the resistor r_m the membrane conductance at this time. The control amplifier maintains the voltage V_{meas} at the command potential by injecting current through the two resistors r_{ig} and r_{eg} . The membrane conductance is very large at the peak of the action potential, so the resistance of the membrane r_m is small in comparison with the extracellular resistance r_b . Obviously, control of the membrane potential is impossible at this time, as Beeler and Reuter (1970) realized in their analysis of the initial currents in a lumped circuit approximation of the clamped membrane. Control is, however, also inadequate if r_m is comparable to r_b in contradistinction to their conclusion that at later times "clamp control is regained." Inspection of their current-voltage plot at these times shows slope resistances of less than 2000 ohms above −30 mv.

A plot of the absolute peak current vs. command potential at the peak of the action potential when r_m is small in comparison with r_b will thus be a straight line with a slope primarily determined by r_b once the threshold voltage is reached. This in-

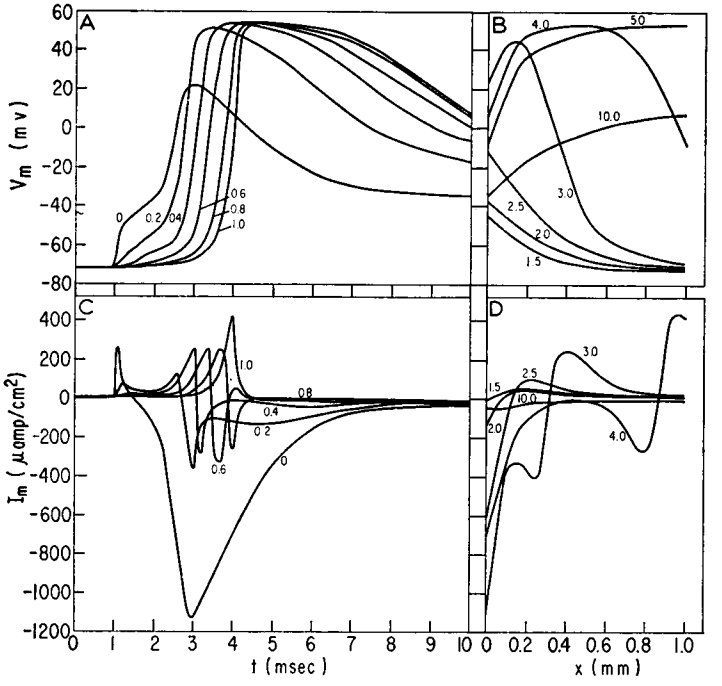

FIGURE 6 Transmembrane potential V_m and current I_m along the "voltage-clamped" cable as a function of time t and distance x from the end nearest the sucrose gap (current injection point). Clamp step from resting potential (−72 mv) to −40 mv applied at t = 1 msec. (A) $V_m(t)$ at six different positions (in millimeters) along the cable. (B) $V_m(x)$ at seven times (in milliseconds) after the clamp step. (C) $I_m(t)$ at the same positions as in A. (D) $I_m(x)$ at the same times as in B.

terpretation means that the shape of the peak current-voltage plot tells us almost nothing about the membrane properties. The slope of the theoretical curve (2.3×10^6 ohms) is, as one would expect, slightly greater than the value of the resistor r_b (1.65×10^6 ohms) and the same is true for the data of Beeler and Reuter. The line intercepts the zero-current axis at a voltage corresponding to the peak height of the action potential. A change in the external sodium concentration, i.e. in the sodium equilibrium potential, causes the line to shift along the voltage axis by an amount equal to the change in equilibrium potential, producing what appears to be a change in the "equilibrium potential" for the peak inward current.

Plots of transmembrane voltage and membrane current as a function of time and position along the preparation are shown in Figs. 6 and 7 for two different clamp steps, demonstrating that for all times considered here, the transmembrane voltage and membrane current vary widely throughout the preparation. The initiation, uniform propagation, and termination of an action potential in the preparation are

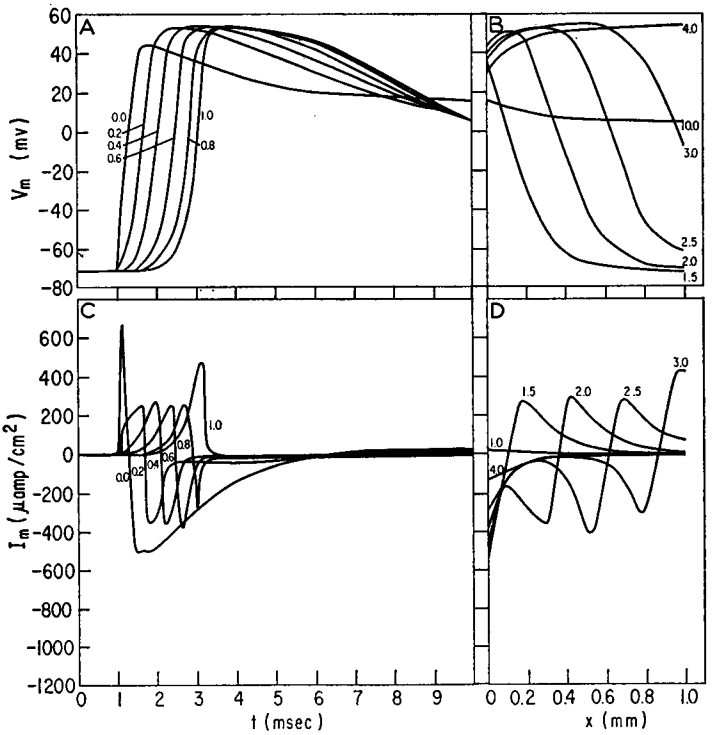

FIGURE 7 Transmembrane potential V_m and current I_m along the "voltage-clamped" cable as a function of time t and distance x from the end nearest the sucrose gap (current injection point). Clamp step from resting potential (−72 mv) to +20 mv applied at t = 1 msec. (A) $V_m(t)$ at six different positions (in millimeters) along the cable. (B) $V_m(x)$ at six times (in milliseconds) after the clamp step. (C) $I_m(t)$ at the same positions as in A. (D) $I_m(x)$ at the same times as in B.

clearly evident in both the membrane voltage and current plots. Note that the records for the two clamp steps are very similar except that it takes longer to initiate the action potential with the smaller clamp step and that the peak membrane current near the current injection point ($X = 0$ in Figs. 6 C and 7 C) is *larger* for the smaller clamp step. The latter is merely a consequence of the fact that the control amplifier sees the larger error voltage for the smaller clamp step.

One can see now how the inclusion of the stray capacitance which no doubt exists across r_{eg} (Fig. 1 B) would insure that at high frequencies even more of the control current would get to r_b without entering the preparation, thus increasing the apparent speed of response. It is perhaps also worthwhile to point out the importance of one other stray capacitance, that from the barrel of the microelectrode to the output of the control amplifier (current pool). Because of the voltage gain of the amplifier, small values of this capacitance can seriously deteriorate the bandwith of the amplifier. For example, a stray capacitance of 10^{-13} farads (0.1 pF), multiplied by an amplifier gain of 1000 and in combination with a microelectrode resistance of 10 mΩ results in an additional time constant of 1 msec, equal to that assumed in the model.

DISCUSSION

Our purpose in this analysis was not to produce a detailed simulation of specific published results and appraise their interpretation, but rather to discover and illustrate the effects of inescapable imperfections of the voltage clamp method as applied to trabeculae of cardiac muscle. It is hoped that analyses of this kind will reveal new ways of circumventing the effects of these imperfections or will direct us to new techniques.

Perhaps the most important lesson to be learned from this analysis is that although the current records and plots that one obtains do not differ very much from those one would get from a perfectly voltage-clamped preparation, one cannot presume that membrane potential control is equally good in both cases. In fact, no semblance of voltage control was achieved in this model. We cannot, of course, be certain that what we have seen here takes place in real voltage-clamped preparations of cardiac muscle; however, one would at least have to eliminate this possibility by additional measurements before placing confidence in other interpretations of the experimental results.

APPENDIX

In order for a negative-feedback control system to be stable, the open-loop gain of the system must be less than one when the phase shift reaches 180° (Milhorn, 1966). Let us assume a control amplifier whose gain vs. frequency characteristics are described by a single-pole low-pass filter with low frequency gain much greater than one. Such an amplifier will exhibit a phase shift of 90° at the frequency where its gain has dropped to unity. Let the controlled element be a lossless delay line of length L (seconds). If the line is lossy, the gain

of the control amplifier can be increased such that the open-loop gain of the system remains greater than one. The phase shift ϕ (degrees) down such a line depends on the frequency f and is 360 Lf degrees. If the total phase shift around the loop is to be less than 180° at the frequency where the gain is one, then ϕ must be less than 90° at this frequency. Since this frequency must also be greater than $1/\tau$, it follows that for a delay line of length L, the time constant τ of the control amplifier must be greater than $4L$ for the closed-loop system to be stable.

This work was supported by U. S. Public Health Service grants HE 12157 and 43004.

Received for publication 18 February 1972 and in revised form 16 June 1972.

REFERENCES

BEELER, G. W., and H. REUTER. 1970. *J. Physiol. (Lond.).* **207**:165.

CHANDLER, W. K., R. FITZHUGH, and K. S. COLE. 1962. *Biophys. J.* **2**:105.

GAGE, P. W., and R. S. EISENBERG. 1969. *J. Gen. Physiol.* **53**:265.

GERALD, C. F. 1970. Applied Numerical Analysis. Addison-Wesley Publishing Company, Inc., Reading, Mass.

HODGKIN, A. L., and A. F. HUXLEY. 1952. *J. Physiol. (Lond.).* **117**:500.

HODGKIN, A. L., and W. A. H. RUSHTON. 1946. *Proc. R. Soc. Lond. B Biol. Sci.* **133**:444.

JOHNSON, E. A., and M. LIEBERMAN. 1971. *Annu. Rev. Physiol.* **33**:479.

JOHNSON, E. A., and J. R. SOMMER. 1967. *J. Cell Biol.* **33**:103.

MASCHER, D., and K. PEPER. 1969. *Pflugers Arch. Eur. J. Physiol.* **307**:190.

MCALLISTER, R. E. 1968. *Biophys. J.* **8**:951.

MILHORN, H. T., JR. 1966. The Application of Control Theory to Physiological Systems. W. B. Saunders Company, Philadelphia.

MITCHELL, A. R. 1969. Computational Methods in Partial Differential Equations. John Wiley & Sons, Inc., New York.

NEW, W., JR. 1971. Voltage control, inward membrane currents and tension in mammalian myocardium. Ph.D. Thesis. University of California, Los Angeles.

OCHI, R. 1970. *Pflugers Arch. Eur. J. Physiol.* **316**:81.

TAYLOR, R. E., J. W. MOORE, and K. S. COLE. 1960. *Biophys. J.* **1**:161.

WEIDMANN, S. 1952. *J. Physiol. (Lond.).* **118**:348.

WEIDMANN, S. 1955. *J. Physiol. (Lond.).* **127**:213.